Journal of Hazardous Materials 189 (2011) 773–786

Contents lists available at ScienceDirect

Journal of Hazardous Materials

journal homepage: www.elsevier.com/locate/jhazmat

Regeneration of natural zeolite polluted by lead and zinc in wastewater treatment systems

Evina Katsou, Simos Malamis*, Myrto Tzanoudaki, Katherine J. Haralambous, Maria Loizidou

School of Chemical Engineering, National Technical University of Athens, 9 Iroon Polytechniou St., Zographou Campus, PC 157 73, Athens, Greece

ARTICLE INFO

Article history:
Received 29 June 2010
Received in revised form
13 December 2010
Accepted 14 December 2010
Available online 22 December 2010

Keywords:
Lead
Zinc
Adsorption
Desorption
Zeolite
Regeneration

ABSTRACT

The aim of this work was to investigate the potential regeneration of natural zeolite which had been contaminated with lead and zinc contained in aqueous solutions, treated secondary effluent and primary treated wastewater. Several desorbing solutions were examined for the removal of Pb(II) and Zn(II) from zeolite and the highest desorption efficiency was obtained for 3 M KCl and 1 M KCl, respectively. The desorption process depended on the type and concentration of the desorbing solution, the metal being desorbed, the mineral selectivity towards the metal and the composition of the liquid medium where the adsorption process had taken place. Successive regeneration cycles resulted in the reduction of desorption efficiency by more than 50% after 9 and 4 cycles for lead and zinc, respectively. Kinetics examination showed that desorption was slower than adsorption, while metal ions which had been easily adsorbed were difficult to be desorbed. Adsorption was characterized by a three-stage diffusion process, while desorption followed a two-stage diffusion process.

1. Introduction

Lead and zinc are among the most common pollutants met in industrial wastewater and are associated with pollution and toxicity problems. Therefore, these metals must be effectively removed from wastewater. Various techniques can be employed for heavy metal removal including precipitation, coagulation – flocculation, electrochemical treatment, chelation, biosorption, adsorption, ion exchange, membrane filtration and solvent extraction [1–3]. These processes have their inherent advantages and limitations in application. Adsorption is a simple and effective process for heavy metal removal, particularly when low-cost adsorbents are employed. Natural zeolites are effectively used in ion exchange processes as sorbents for Pb(II) and Zn(II) removal, owing to their high reserves, advantageous ion exchange capacities, high metal selectivity and low-cost. The adsorption capacities reported for natural clinoptilolite and Fe-over-exchanged clinoptilolite for Zn(II) uptake from drinking water were 71.3 mg/g and 94.8 mg/g, respectively [4]. Castaldi et al. [5] found that the maximum adsorption capacity of natural zeolite for Pb(II), Zn(II) and Cd(II) in batch reactors was 246.6 mg/g, 96.1 mg/g and 130.4 mg/g, respectively. Günay et al. [6] found that the adsorption capacity of raw and pre-treated clinoptilolite for Pb(II) removal from aqueous solutions was 80.9 mg/g and 122.4 mg/g, respectively. Sprynskyy et al. [7] determined the sorption capacity of clinoptilolite for Pb(II) in multi-component aqueous solutions to be 27.8 mg/g. Cincotti et al. [8] found that the adsorption capacity of Sardinian natural zeolite was 55.9–248.6 mg/g for lead and 6.5 mg/g for zinc. Oter and Akcay [9] concluded that Turkish clinoptilolite had an adsorption capacity of 47.5–151.3 mg/g for lead and 7.1–16.4 mg/g for zinc. The findings of the above studies reveal that natural zeolite is an effective adsorbent for Zn(II) and Pb(II) uptake. A drawback of the adsorption process is that the mineral is usually not recycled. Sorbent regeneration results in metal recovery and reuse of the adsorbent. Such studies are therefore important for future practical use of the mineral and can render adsorption an economically more attractive treatment method [10].

A small number of studies have been performed on the regeneration of clinoptilolite after Zn(II) and Pb(II) adsorption. Gedik and Imamoglu [10] tested four different chemicals (1 M NaCl, KCl, $CaCl_2$ and HCl) for clinoptilolite regeneration and cadmium recovery, with NaCl exhibiting the highest adsorbent regeneration efficiency (72–97%). Regeneration of clinoptilolite by 95% as well as Pb(II) recovery was obtained using 30 g/l NaCl at pH 11.5 in a fixed bed column [11]. Eight regeneration cycles of natural zeolite from Pb(II) were conducted in fixed bed columns by employing 15 g/l $NaNO_3$ as desorbing solution, achieving 3–4 times smaller volume of regeneration solution per cycle compared to the metal solution

* Corresponding author. Tel.: +30 210 772 3108; fax: +30 210 772 3285.
E-mail addresses: ekatsou@yahoo.gr (E. Katsou), malamis.simos@gmail.com (S. Malamis), mirtotz@hotmail.com (M. Tzanoudaki), harjo@chemeng.ntua.gr (K.J. Haralambous), mloiz@orfeas.chemeng.ntua.gr (M. Loizidou).

0304-3894/$ – see front matter © 2010 Elsevier B.V. All rights reserved.
doi:10.1016/j.jhazmat.2010.12.061

volume [12]. Cui et al. [13] studied the adsorption/desorption of zinc on/from clinoptilolite in a laboratory slurry bubble column using NaCl as desorbent accomplishing a desorption efficiency of 56%. Li et al. [14] investigated the desorption of Zn(II) from clinoptilolite and found that EDTA was the most effective desorbing medium followed by NaCl.

The aim of this work is to investigate the regeneration of zinc and lead contaminated clinoptilolite with the use of suitable desorbing solutions. This way the mineral can be employed several times for the removal of heavy metals from wastewater. Also, heavy metals can be diverted from a wastewater stream to a low-volume desorbing solution that can be easily handled.

2. Materials and methods

2.1. Adsorbent, chemicals and liquid media employed

Natural (85% clinoptilolite), Greek zeolite was the adsorbent that was employed in this work. The mineral was obtained by S&B Industrial Minerals S.A. Zeolite was sieved to the desired size (1.0–1.4 mm), washed with deionised water, dried at 80 °C for at least 24 h and stored in a desiccator until its use. Zeolite was used in its natural form without any chemical modification in order to reduce the overall cost of the process.

The chemical composition of zeolite was obtained by X-ray fluorescence analysis (XRF)-Wavelength Dispersive (model ARL, ADVANT XP) and the crystalline phases were determined by a conventional Bragg-Brentano X-ray diffraction (XRD) using a Siemens D5000 powder unit with Cu-Kα source. The reagents employed for the experiments were of analytical grade and were supplied by Merck. Metal solutions were prepared by dissolving the appropriate amount of salts [$Pb(NO_3)_2$ and $Zn(NO_3)_2{\cdot}6H_2O$] in deionised water. Desorption experiments were performed using HNO_3 at the concentrations of 5% and 10%, NaCl, KCl and NH_4Cl at the concentrations of 0.1 M, 0.5 M, 1 M, 3 M and 5 M.

The adsorption experiments were conducted in three different liquid media (i.e. aqueous solutions, secondary effluent and primary treated wastewater). The secondary effluent was collected from the outflow of a Membrane Bioreactor (MBR) system treating municipal wastewater. Primary treated wastewater was collected from the overflow of the primary sedimentation tank of a municipal wastewater treatment plant. The parameters of pH, total suspended solids (TSS) and volatile suspended solids (VSS) were determined using standard methods [15]. Chemical oxygen demand (COD), total nitrogen (TN), nitrate nitrogen (NO_3-N), ammonium nitrogen (NH_4-N) were measured in the photometer NOVA 60 using suitable Merck kits. Na^+, Ca^{2+}, Mg^{2+}, K^+, Pb^{2+} and Zn^{2+} were measured with atomic absorption spectroscopy (Varian model AA240FS).

2.2. Batch adsorption studies

The adsorption experiments were conducted in batch reactors (500 ml) where the three liquid media (i.e. aqueous solutions, MBR permeate and primary treated wastewater) were enriched with Pb(II) and Zn(II) ions in order to have a fixed initial metal concentration in the solution of 320 mg/l. The zeolite concentration added to the solution was fixed at 10 g/l. The solution pH was adjusted at 3.5 using HNO_3 in order to avoid precipitation. The batch reactors were kept at room temperature (25 °C) without any agitation until equilibrium was reached (i.e. for 10 h). Agitation was not employed in order to avoid the breakdown of the chosen mineral granular size. Moreover, it was found from preliminary experimental work that the difference in the metal uptake obtained in an agitated (250 rpm) and a non-agitated system was not significant provided that adequate time was allowed for the adsorption process to develop.

Then the solutions were filtered through Whatman membranes with pore size 0.45 μm and the zeolite retained by the membrane was collected in order to conduct the desorption experiments. The filtrate was measured in AAS for its Pb(II) and Zn(II) content. To examine the system adsorption kinetics the above experiments were conducted with sampling taking place at regular intervals for a period of more than 10 h. This way the variation of the metal uptake with time was determined. Kinetics examination was conducted for all three liquid media (i.e. aqueous solution, MBR permeate and wastewater). The total sampling volume was always less than 2% of the total solution volume.

2.3. Batch desorption studies

The zeolite previously used in the adsorption experiments (i.e. polluted with lead or zinc ions) was gently washed with deionised water to remove impurities from its surface, was dried at 80 °C for at least 24 h and placed in a desiccator until further use. Then the zeolite was placed into the desorbing solution (HNO_3, NaCl, KCl and NH_4Cl) in a batch process. The solution remained without any agitation at 25 °C until equilibrium was reached (i.e. for 20 h). The solution pH was not adjusted since the addition of HNO_3 or NaOH would introduce competitive cations into the solution and the effectiveness of the pure desorbing solution would not be observed. Then the solutions were filtered through Whatman membranes (0.45 μm) and the zeolite was collected; the filtrate was analyzed for its Zn(II) and Pb(II) content. Desorption kinetic studies were conducted as follows: zeolite samples polluted with lead and zinc in water, MBR permeate and wastewater, were placed in the desorbing solution exhibiting the highest desorption efficiency (i.e. 3 M KCl for lead and 1 M KCl for zinc). Samples from the desorbing solution were collected at regular intervals and were analyzed for their metal content. The total duration of this process was 20 h. The total sampling volume was always less than 2% of the total solution volume.

2.4. Zeolite regeneration

The solutions exhibiting the highest recovery for each metal were used to examine the mineral regeneration potential (i.e. 3 M KCl for lead and 1 M KCl for zinc). Regeneration was tested by conducting successive Pb(II) and Zn(II) adsorption/desorption cycles. Once the desorption process had reached equilibrium the mineral was gently washed to remove the desorbing solution from its surface, it was then dried at 80 °C and placed in a dessicator until the next adsorption/desorption cycle. During each adsorption/desorption cycle no other treatment took place in order to minimize the overall cost of the treatment process. The repeated cycles were conducted for all three liquid media under examination. At the completion of each adsorption/desorption cycle the regenerated clinoptilolite samples were used for further Zn(II) and Pb(II) adsorption and desorption following the experimental procedure described in Sections 2.2 and 2.3.

It must be noted that for each set of experiments three replicates were conducted.

3. Theory

3.1. Adsorption

The amount of metal adsorbed on zeolite (clinoptilolite) per unit mass of adsorbent, q_a (mg/g) at equilibrium is given by:

$$q_a = \frac{(C_{initial} - C_{final})}{m} V \quad (1)$$

where $C_{initial}$ (mg/l) is the initial metal concentration in the solution, C_{final} (mg/l) is the liquid phase metal concentration at the completion of the adsorption experiment (i.e. equilibrium conditions), m (g) is the mass of the adsorbent employed and V (l) is the liquid volume where the adsorption process takes place.

3.2. Desorption

The metal content in the desorbing solution at the completion of the desorption experiment (i.e. equilibrium conditions), represents the amount of metal that has been desorbed. Desorption efficiency is given as a percentage of the amount of metal desorbed (i.e. released into the solution) per unit mass of desorbent Q_d (mg/g), to the amount of metal adsorbed onto the mineral per unit mass of adsorbent, q_a (mg/g) at equilibrium:

$$(\%)\,\text{Desorption efficiency} = \frac{Q_d}{q_a} \times 100 \quad (2)$$

The amount of each metal desorbed from zeolite into the solution per unit mass of desorbent, Q_d (mg/g) at equilibrium is calculated by:

$$Q_d = \frac{C_{desorbed}}{m} V' \quad (3)$$

where $C_{desorbed}$ (mg/l) is the liquid phase metal concentraion detected in the desorbing solution at the end of the desorption experiment (i.e. equilibrium conditions) and V' (l) is the volume of the desorbing solution.

3.3. System kinetics and mechanisms

Existing models were employed to describe the adsorption and desorption processes of zinc and lead on and from zeolite. A wide range of reaction and diffusion models have been applied to describe the metal-ion sorption and desorption [16]. The pseudo-first-order, the pseudo-second-order, the Elovich equation as well as diffusion equations (Fick's law) have been successfully applied to describe the adsorption/desorption of cations on/from minerals. Every model has its own limitations and ability to fit the kinetic data. The models do not work ideally, nor can one propose mechanisms based on one fit alone [17]. In the present study several existing models have been applied to study the adsorption and desorption processes. The reaction and diffusion models were compared to the experimental data and their parameters were determined. The models employed to describe the adsorption/desorption processes were the pseudo-first-order, the pseudo-second-order, the Elovich model as well as the diffusion models of external mass transfer, intraparticle diffusion, Reichenberg's equation, Fick's law for long adsorption times (i.e. homogeneous diffusion) and Vermeulen's approximation. The pseudo-first-order, pseudo-second-order, Elovich and external mass transfer models were solved using non-linear regression analysis, by minimizing the error Δq (%) using Solver of Microsoft Excel 2007. The other models were solved using linear regression analysis.

3.3.1. Pseudo-first-order model

The integral, non-linear form of the pseudo-first-order model is given by [18,19]:

$$q_{ta} = q_a\,(1 - e^{-k_{1a}t}) \quad (\text{for adsorption}) \quad (4.1)$$

$$q_{td} = (q_{0d} - q_d)\,e^{-k_{1d}t} + q_d \quad (\text{for desorption}) \quad (4.2)$$

where q_a and q_d (mg/g) are the solid phase equilibrium concentrations of the metal at the completion of adsorption and desorption respectively, q_t (mg/g) is the solid phase metal concentration at time t, q_{0d} (mg/g) refers to the solid phase metal concentration at t = 0 of the desorption process, k_1 (min^{-1}) is the rate constant of the model and the subscripts a and d refer to adsorption and desorption respectively.

3.3.2. Pseudo-second-order model

The integral, non-linear form of the pseudo-second-order model is given by [19,20]:

$$q_{ta} = \frac{q_a^2 k_{2a} t}{1 + q_a k_{2a} t} \quad (\text{for adsorption}) \quad (5.1)$$

$$q_{td} = q_d + \frac{q_{0d} - q_d}{1 + (q_{0d} - q_d)\,k_{2d} t} \quad (\text{for desorption}) \quad (5.2)$$

where k_2 ($g\,mg^{-1}\,min^{-1}$) is the rate constant of the model. Chemical sorption is the rate limiting step in the pseudo-second-order model.

3.3.3. Elovich model

The integral, non-linear form of the Elovich equation is given by [21]:

$$q_{ta} = \frac{1}{\beta} \ln(1 + \alpha\beta t) \quad (6)$$

where α is the initial adsorption rate ($mg\,g^{-1}\,min^{-1}$) and β is a constant related to desorption (g/mg). When the equation is applied for desorption, q_{ta} is replaced by Q_{td} where the latter represents the amount of metal that is desorbed (i.e. released into the liquid) at time t.

3.3.4. Diffusion models

Three main steps are involved in the solid-liquid sorption process between the metal ions and the adsorbent:

(a) The metal ions are transferred from the bulk solution to the surface of the liquid boundary layer surrounding the particle and then diffuse across the boundary layer to the surface of the adsorbent. The latter is known as film diffusion.
(b) The active sites on the surface of the adsorbent capture the metal ions.
(c) The metal ions are transferred within the pores of the adsorbent. This is known as intraparticle diffusion, occurring either as pore diffusion or as a solid surface diffusion mechanism.

The second step occurs at a very high rate and does not control the process. Thus, either intraparticle diffusion or film diffusion is the rate-controlling step.

The usual approach to determine whether the adsorption process is governed by intraparticle diffusion is to plot the intraparticle diffusion model. If the plot is linear and passes through the origin then intraparticle diffusion is the controlling mechanism. This model is given by [22]:

$$q_{ta} = k_i t^{0.5} \quad (7.1)$$

where k_i ($mg\,g^{-1}\,min^{-1/2}$) is the rate constant of intraparticle diffusion.

A similar form is given for the desorption process (i.e. parabolic diffusion model):

$$Q_{td} = k_{id} t^{0.5} + c \quad (7.2)$$

where k_{id} ($mg\,g^{-1}\,min^{-1/2}$) is the equation rate constant and c is a constant.

Reichenberg's model is given by the following equations [23]:

$$\text{for } F \le 0.85 \quad Bt = 2\pi - \frac{\pi^2 F}{3} - 2\pi\sqrt{\left(1 - \frac{\pi F}{3}\right)} \quad (8)$$

$$\text{for } F > 0.85 \quad Bt = -0.4977 - \ln(1 - F) \quad (9)$$

where:

$$B = \frac{\pi^2 D_{\text{eff}}}{r^2} \tag{10}$$

$$F = \frac{q_{\text{ta}}}{q_{\text{a}}} \tag{11}$$

where F is the fractional attainment of equilibrium at time t, D_{eff} (m^2/s) is the effective diffusion coefficient of metal ions in the adsorbent phase, r (m) is the radius of adsorbent particle assumed to be spherical.

At long adsorption times, the following expression holds from Fick's law (i.e. homogeneous diffusion) [24]:

$$\ln(1-F) = \ln\left(\frac{6}{\pi^2}\right) + \left(\frac{-D_{\text{eff}}\pi^2}{r^2}\right) t \tag{12}$$

To determine D_{eff}, $\ln(1-F)$ is plotted against time t.

Vermeulen's approximation for adsorption onto spherical particles for the whole range of $0 \le F \le 1$ is given by [24]:

$$F = \left[1 - \exp\left(\frac{-\pi^2 D_{\text{eff}} t}{r^2}\right)\right]^{1/2} \tag{13}$$

Eq. (13) in its linear form becomes:

$$\ln\left(\frac{1}{1-F^2}\right) = \frac{\pi^2 D_{\text{eff}} t}{r^2} \tag{14}$$

To determine D_{eff}, $\ln(1/(1-F^2))$ is plotted against time t.

The integrated form of the external mass transfer model is given by [25–27]:

$$\ln \frac{C_{\text{initial}} - C_{\text{s}}}{C_t - C_{\text{s}}} = k_{\text{f}} a_{\text{m}} t \tag{15}$$

where

$$a_{\text{m}} = \frac{6 m_{\text{a}}}{d_{\text{p}} \rho_{\text{b}}} \tag{16}$$

where C_{s} (mg/l) is the metal concentration at the surface of adsorbent, C_t (mg/l) is the liquid phase metal concentration at time t, a_{m} ($m^2\ m^{-3}$) is the specific area of the adsorbent, m_{a} (g/l) is the adsorbent concentration, k_{f} ($m\ min^{-1}$) is the mass transfer coefficient between the bulk solution and the solid surface, d_{p} (m) is the average particle diameter, ρ_{b} (g/l) is the adsorbent bulk density. This model describes the movement of the solute from the liquid phase to the surface of the adsorbent. The value of k_{f} was determined by non-linear regression analysis.

3.4. Error analysis

The percentage error Δq was obtained using the following equation:

$$(\%)\ \Delta q = 100 \times \sqrt{\frac{\sum_{i=1}^{n}((q_{\text{ta exp}} - q_{\text{ta model}})/q_{\text{ta exp}})_i^2}{n-1}} \tag{17}$$

where $q_{\text{ta exp}}$ and $q_{\text{ta mod}}$ (mg/g) are the equilibrium adsorption capacities obtained experimentally and predicted by the model respectively and n is the number of data points. The same formula was also applied for desorption using q_{td}. In the case of the external mass transfer model the above equation was applied for C_{t}.

4. Results and discussion

In this Section the experimental results obtained are discussed and assessed. This includes (i) the characterization of zeolite, (ii) the determination of the amount of Pb(II) and Zn(II) adsorbed on zeolite and the examination of the associated adsorption kinetics, (iii) the evaluation of the performance of desorbing solutions used for mineral regeneration and metal recovery and the assessment of the associated desorption kinetics, (iv) the assessment of the regeneration potential of the metal-loaded clinoptilolite to sustain its adsorption potential in successive adsorption/desorption cycles. The results of this study can be used for the design of a sustainable, cost-effective wastewater treatment system, enabling the recovery of both the sorbent and the metal.

Table 1
Normalized chemical composition of natural zeolite obtained by XRF.

Substances	(%)
SiO_2	77.08
Al_2O_3	13.08
Fe_2O_3	0.97
CaO	3.68
Na_2O	0.32
MgO	0.76
K_2O	4.00
TiO_2	0.11

4.1. Mineral characterization

The major constituents of zeolite were silica (SiO_2) and alumina (Al_2O_3) (Table 1). The zeolite structure indicated the presence of mobile ions such as Ca^{2+}, Na^+ and K^+. The molar ratio of SiO_2/Al_2O_3 was 10:1 indicating significant theoretical ion exchange capacity. Zeolite was characterized by poor sodium and magnesium content and higher calcium and potassium content. According to the data presented in Table 1 the theoretical cation exchange capacity (CEC) of zeolite was calculated to be equal to 2.37 meq/g based on the Al content, while the measured CEC of zeolite was 1.88 meq/g according to the NH_4Ac method [28].

Natural zeolite mainly consisted of Na-form and Ca-form clinoptilolite with some quantities of feldspar, quartz, illite and chabazite. Due to overlapping of diffraction maxima, the presence of some minor contents could not be included. Fig. 1 shows the forms of clinoptilolite that dominate the structure of the natural zeolite.

4.2. Adsorption studies

Adsorption was conducted in three liquid media: (a) aqueous solutions, (b) MBR permeate and (c) primary treated wastewater. The characteristics of wastewater and MBR permeate are summarized in Table 2. Primary treated wastewater was typical municipal wastewater, containing significant concentrations of ammonium

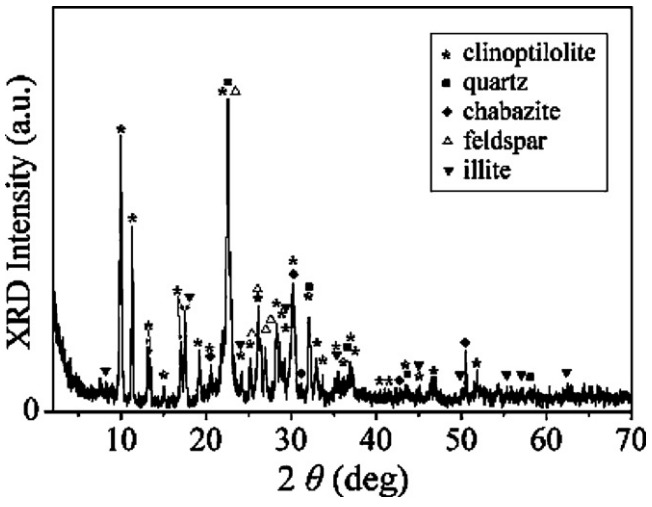

Fig. 1. X-ray diffraction patterns of natural zeolite.

Table 2
Composition of primary treated wastewater and MBR permeate.

Parameter	Primary treated wastewater	MBR permeate
pH	7.2 (7.0–7.6)	7.1 (6.9–7.4)
TSS (mg/l)	252 (150–325)	<1
VSS (mg/l)	195 (105–305)	–
COD (mg/l)	549 (465–619)	21 (16–27)
NH_4-N (mg/l)	53 (48–59)	<0.5
NO_3-N (mg/l)	<0.5	45 (39–48)
TN (mg/l)	69 (64–75)	50 (45–54)
Na^+ (mg/l)	196 (101–310)	135 (93–205)
Ca^{2+} (mg/l)	213 (145–295)	147 (85–251)
Mg^{2+} (mg/l)	37 (17–56)	26 (11–46)
K^+ (mg/l)	5 (2–16)	2 (0–8)

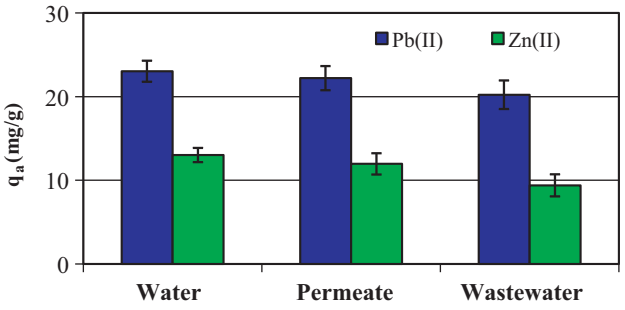

Fig. 2. Amount (mg/g) of lead and zinc adsorbed on zeolite in aqueous solutions, MBR permeate and wastewater at pH 3.5.

that compete with heavy metals for the available mineral adsorption sites. The MBR permeate was characterized by very low organic matter and significant nitrate concentration. Both the wastewater and the MBR permeate contained other cations such as calcium, sodium and magnesium which compete with heavy metals for the available mineral sites.

The amount of zinc and lead ions adsorbed on zeolite is given in Fig. 2. Mineral performance was higher for Pb(II) compared to Zn(II) in all liquid media, which also agrees with previous findings [5,8,9,29]. Table 3 compares the amount of lead and zinc adsorbed on zeolite in this work with the adsorption capacities of minerals (i.e. zeolite, vermiculite, bentonite and kaolinite) reported in the literature for lead and zinc removal [5,7–9,29–46]. The zeolite used in the present study exhibited higher [33,37,42,46] or comparable [38,40] performance for Pb(II) and Zn(II) removal compared to that of several cases reported in the literature. The amount of lead adsorbed on zeolite was comparable to the one reported by Sprynskyy et al. [7] and Turkman et al. [30]. However, it was lower than most of the zeolite adsorption capacities reported in the literature. The low amount of lead adsorbed is attributed to the relatively low ratio of the available lead concentration to the mineral concentration, thus limiting the mineral potential for higher lead uptake. Also, the acidic nature of the solution (pH 3.5) resulted in more protons which competed with the Pb(II) ions for the available adsorption sites of the mineral. These two factors limited lead adsorption. Zinc adsorption on zeolite was found to be comparable to that obtained in other studies [9,45]. Considering the low cost and the regeneration potential of natural zeolite, it can be adopted as an effective adsorbent for the removal of lead and zinc ions from various industrial wastewater streams.

The adsorption of Pb(II) and Zn(II) on zeolite was found to be reversible. The zeolite adsorption and ion exchange capacity towards metal cations was influenced by the composition of the solution where the adsorption process took place. The adsorption of lead and zinc on zeolite in the three solutions followed the order aqueous solution > permeate > wastewater. This is reasonable since wastewater contained NH_4^+ and other cations that competed with lead or zinc ions for the available adsorption sites. Consequently, adsorption of heavy metals on zeolite was lower in wastewater. The MBR permeate contained Ca^{2+}, Mg^{2+}, Na^+ and K^+ that competed to some extent with lead and zinc during the adsorption process, as opposed to aqueous solutions where these cations were not present. Zinc was more suppressed than lead by the presence of competitive cations in wastewater. The cation selectivity sequence for Na-form clinoptilolite obtained by Langella et al. [47] was $NH_4^+ > Pb^{2+} > Na^+ > Cd^{2+} > Cu^{2+} \approx Zn^{2+}$, indicating that clinoptilolite exhibited similar selectivity towards NH_4^+ and Pb^{2+} and significantly lower exchange capability for Zn^{2+}. It seems that the high Si/Al ratio of clinoptilolite resulted in a low anionic field that favoured the exchange of monovalent cations present in wastewater and MBR permeate as opposed to divalent cations. Lead, due to its lower hydration energy, did not obey this rule and thus natural zeolite had significantly higher selectivity towards lead than zinc [47].

Kinetics examination was conducted for the adsorption of lead and zinc ions on minerals. In Fig. 3 the amount of lead and zinc adsorbed on zeolite in aqueous solutions, MBR permeate and wastewater at pH 3.5 is given with time. It is evident that higher lead adsorption on zeolite occurred compared to zinc. Lead ions tended to attain equilibrium faster than zinc ions in all three liquid media. At the early stages of the adsorption process the metal ions were more rapidly adsorbed on the mineral in aqueous solutions than in wastewater and permeate and tended to reach equilibrium faster. Lead and zinc adsorption on zeolite in aqueous solution exhibited the highest performance compared to that of the other two liquid media. Equilibrium was reached at approximately 240 min for lead and 360 min for zinc.

The experimental data were compared against the pseudo-first-order, the pseudo-second-order, and the Elovich reaction kinetic models. Table 4 shows the equation constants and the percentage error Δq (%) obtained for the models under investigation. In most cases the Elovich model had the smallest error. The pseudo-second-order model also closely matched the experimental results having lower error than the pseudo-first-order model. In addition, the predicted q_a of the pseudo-second-order model was closer to the experimental one than that of the pseudo-first-order model. The experimental data were further compared to the external mass transfer and the intraparticle diffusion models. The external mass transfer model is only applicable during the initial stages of the process, as it does not consider the adsorption inside the mineral pores. The external mass transfer coefficient k_f was determined which has a physical meaning, as it explains the transfer of metal ions from the solution through the boundary layer to the external mineral surface. The value of k_f obtained for lead adsorption was significantly higher than that of zinc, indicating higher mass transfer rate of lead ions towards the sorbent surface for all three liquid media. In all cases the metal concentration at the surface of the adsorbate C_s was found to be negligible. After the initial stages of adsorption, the external mass transfer model could not be applied as it deviated considerably from the experimental data.

In Fig. 4 the intraparticle diffusion model was plotted for the obtained experimental data. It is seen that a multi-linear plot was obtained and three distinct stages were identified which indicated that three different diffusion steps took place. The gradient of each linear part provides an indication of the rate of adsorption. The diffusion rate decreased with increasing contact time. In the first stage, the rate of metal uptake was higher than that in the other stages. The initial adsorption of zinc and lead on the mineral developed at a lower rate in wastewater and permeate compared to water due to the increased competition among zinc or lead ions and other cations for the available adsorption sites. Moreover, the rate of lead diffusion on zeolite was higher than that of zinc. In the second stage a more gradual metal uptake occurred. The final stage was charac-

Table 3
Comparison of the amount of Pb(II) and Zn(II) adsorbed on various minerals.

Metal adsorbed	Adsorbent	Amount of metal adsorbed (mg/g)	Reference
Pb	Natural zeolite	23.03	Present study[a]
Zn	Natural zeolite	13.02	Present study[a]
Pb	Natural zeolite	246.57	[5]
Zn	Natural zeolite	96	[5]
Pb	Clinoptilolite	27.76	[7]
Pb	Sardinian natural zeolite	27.97–124.32	[8]
Zn	Sardinian natural zeolite	3.27	[8]
Pb	Turkish clinoptilolite	23.73–75.63	[9]
Zn	Turkish clinoptilolite	3.53–8.21	[9]
Pb	Scolecite	5.80	[29]
Zn	Scolecite	2.09	[29]
Pb	Bigadic clinoptilolite	23	[30]
Zn	Bigadic clinoptilolite	24	[30]
Pb	Clinoptilolite	166	[31]
Pb	Raw clinoptilolite	80.9	[32]
Pb	Pretreated clinoptilolite	122.4	[32]
Pb	TBA–kaolinite	3.2	[33]
Pb	TBA–montmorillonite	10.7	[33]
Pb	ZrO–kaolinite	4.4	[33]
Pb	ZrO–montmorillonite	16.9	[33]
Pb	Vermiculite	94.61	[34]
Pb	Vermiculite	1.64	[35]
Zn	Vermiculite	3.88	[35]
Pb	Bentonite	52.6	[36]
Pb	Native bentonite	6.49	[37]
Pb	Activated bentonite	2.32	[37]
Pb	Raw bentonite	16.7	[38]
Pb	Iron bentonite	22.2	[38]
Pb	Mg-coated bentonite	31.9	[38]
Zn	Na-enriched bentonite	57.44	[39]
Zn	Natural bentonite	30.70	[39]
Zn	Modified montmorillonite	13.27	[40]
Zn	Bentonite	80.64	[41]
Pb	Bentonite	7.56	[42]
Pb	Kaolinite	4.50	[42]
Zn	Bentonite	9.12	[42]
Zn	Kaolinite	3.05	[42]
Zn	Bentonite	36.63	[43]
Zn	Natural clinoptilolite	3.47	[44]
Zn	Turkish clinoptilolite	8.76	[45]
Zn	Kaolinite	1.80	[46]
Zn	Ball clay	2.88	[46]

[a] The given amount of metal adsorbed was obtained in aqueous solutions.

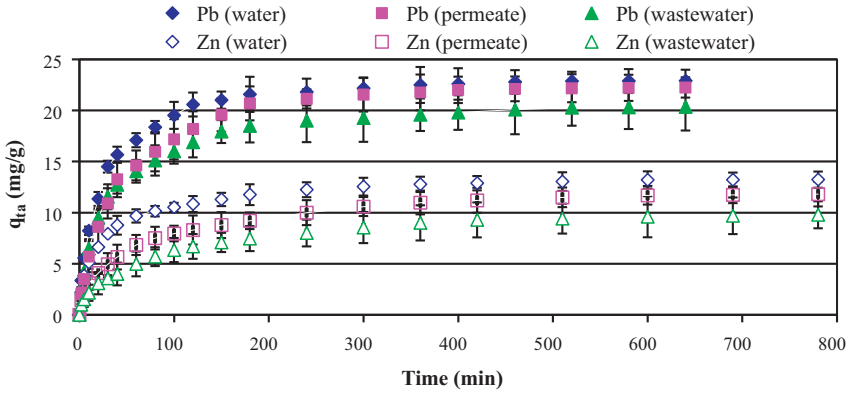

Fig. 3. Amount (mg/g) of lead and zinc adsorbed on zeolite in aqueous solutions, MBR permeate and wastewater at pH 3.5.

terized by a very low adsorption rate since equilibrium had almost been reached. The findings from the application of the intraparticle diffusion model and the external mass transfer model indicate that both intraparticle and film diffusion were important, with the latter being dominant only at the initial stages of adsorption. The experimental data were further compared to the diffusion equations of Reichenberg, Vermeulen and an expression of homogeneous diffusion at long adsorption times, through which it was possible to determine the effective diffusion coefficient (D_{eff}) given in Table 4. D_{eff} was always higher in the case of lead compared to zinc, indicating more effective lead diffusion. In addition, D_{eff} was higher in aqueous solutions compared to MBR permeate and wastewater, indicating that the diffusion process was influenced by the type of the solution.

Table 4
Kinetic parameters for the adsorption of Pb(II) and Zn(II) onto zeolite in aqueous solutions, permeate and wastewater.

Liquid medium	Pseudo-first-order			Pseudo-second-order			Elovich			Experimental
	k_{1a} (min^{-1})	q_a ($mg\,g^{-1}$)	Δq (%)	k_{2a} ($g\,mg^{-1}\,min^{-1}$)	q_a ($mg\,g^{-1}$)	Δq (%)	α ($mg\,g^{-1}\,min^{-1}$)	β ($g\,mg^{-1}$)	Δq (%)	q_{ea} ($mg\,g^{-1}$)
Pb(II)										
Water	0.0535	20.68	13.47	0.00282	22.81	6.95	2.655	0.233	7.88	22.90
Permeate	0.0323	20.07	13.80	0.00158	22.80	7.74	1.208	0.203	7.75	22.25
Wastewater	0.0464	17.79	14.63	0.00270	19.89	7.87	1.806	0.254	6.41	20.34
Zn(II)										
Water	0.0653	11.30	16.07	0.00650	12.42	8.88	2.093	0.454	5.20	13.23
Permeate	0.0328	9.54	21.49	0.00372	10.74	15.01	0.784	0.464	6.28	11.82
Wastewater	0.0248	7.94	22.52	0.00337	8.97	16.34	0.469	0.532	7.97	9.79

Liquid medium	External mass transfer		Intraparticle diffusion						External mass transfer		Intraparticle diffusion					
	Pb(II)		Pb(II)						Zn(II)		Zn(II)					
	k_f ($m\,min^{-1}$)	Δq (%)	k_{i1} ($mg\,g^{-1}\,min^{-1/2}$)	k_{i2} ($mg\,g^{-1}\,min^{-1/2}$)	k_{i3} ($mg\,g^{-1}\,min^{-1/2}$)	R_1^2	R_2^2	R_3^2	k_f ($m\,min^{-1}$)	Δq (%)	k_{i1} ($mg\,g^{-1}\,min^{-1/2}$)	k_{i2} ($mg\,g^{-1}\,min^{-1/2}$)	k_{i3} ($mg\,g^{-1}\,min^{-1/2}$)	R_1^2	R_2^2	R_3^2
Water	4.696×10^{-4}	6.95	2.5689	1.0897	0.1403	0.999	0.999	0.919	1.785×10^{-4}	6.63	1.3812	0.3612	0.0777	0.990	0.999	0.911
Permeate	2.866×10^{-4}	4.09	2.0314	1.0793	0.1306	0.991	0.999	0.916	0.910×10^{-4}	4.29	0.8728	0.3689	0.0935	0.998	0.999	0.937
Wastewater	3.169×10^{-4}	5.71	2.1502	0.8799	0.1616	0.998	0.999	0.966	0.498×10^{-4}	3.71	0.6268	0.2860	0.0689	0.999	0.999	0.989

Liquid medium	Reichenberg				Homogeneous diffusion $t \to \infty$				Vermeulen			
	Pb(II)		Zn(II)		Pb(II)		Zn(II)		Pb(II)		Zn(II)	
	D_{eff} (m^2/s)	R^2	D_{eff} (m^2/s)	R^2	D_{eff} (m^2/s)	R^2	D_{eff} (m^2/s)	R^2	D_{eff} (m^2/s)	R^2	D_{eff} (m^2/s)	R^2
Water	6.14×10^{-12}	0.9835	4.92×10^{-12}	0.9805	6.30×10^{-12}	0.9776	5.05×10^{-12}	0.9769	6.20×10^{-12}	0.9799	4.92×10^{-12}	0.9754
Permeate	6.08×10^{-12}	0.9962	3.95×10^{-12}	0.9926	6.33×10^{-12}	0.9922	4.13×10^{-12}	0.9928	5.84×10^{-12}	0.9964	3.65×10^{-12}	0.9884
Wastewater	5.35×10^{-12}	0.9766	3.53×10^{-12}	0.9963	5.53×10^{-12}	0.9730	3.77×10^{-12}	0.9945	5.23×10^{-12}	0.9733	3.28×10^{-12}	0.9936

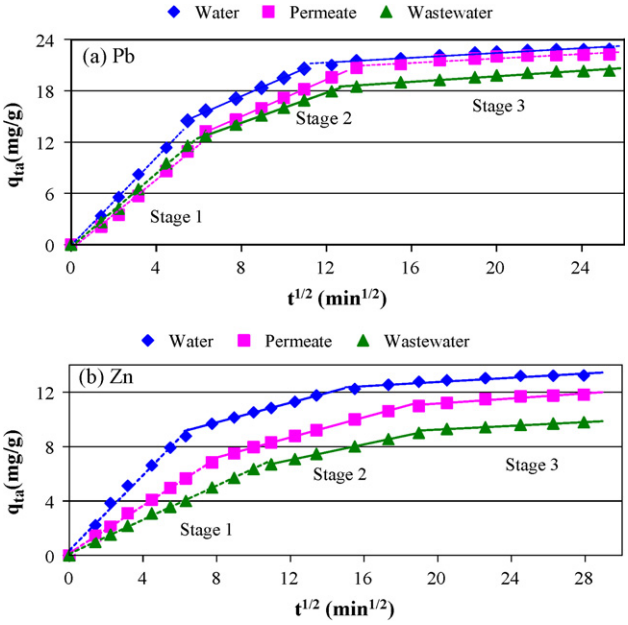

Fig. 4. Plots of (a) lead and (b) zinc adsorbed on zeolite versus the square root of time in aqueous solutions, MBR permeate and wastewater at pH 3.5.

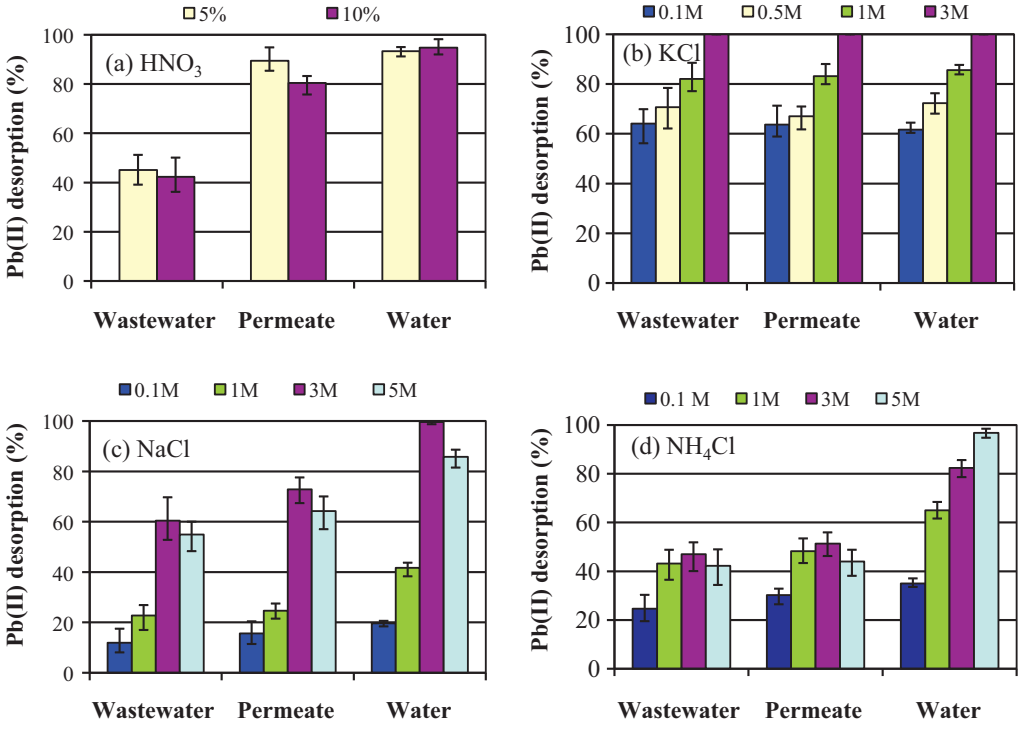

Fig. 5. Percentage desorption efficiency of Pb(II) achieved by (a) HNO_3, (b) KCl, (c) NaCl and (d) NH_4Cl.

4.3. Desorption studies

Desorption studies were conducted to select the optimum desorbing solution to be employed in successive regeneration cycles. Desorption of lead and zinc from natural zeolite was examined in batch reactors for four (4) different desorbing solutions. In Fig. 5 the percentage desorption efficiency of lead is shown when the solutions of HNO_3, KCl, NaCl and NH_4Cl were employed. The use of HNO_3 could achieve effective desorption of lead adsorbed onto zeolite in aqueous solutions, showing that H^+ are competitive and can replace the heavy metal ions from zeolite. Nevertheless, HNO_3 was not effective for desorption of lead from zeolite eluted from primary wastewater. KCl was very effective for lead desorption, irrespective of the liquid medium in which adsorption had taken place. The desorption efficiency was 60–80% when KCl was added at the concentrations of 0.1 M and 1 M, while it reached >99.5% for 3 M in all three liquid media. The desorption efficiency was high (>80%) when 3 M and 5 M NaCl and NH_4Cl were employed only in aqueous solutions, while it was limited in the other two liquid media.

The lower desorption efficiency obtained for zeolite eluted from wastewater is attributed to the presence of significant concentrations of ammonium, sodium and potentially other cations. The adsorption process resulted in the uptake of these ions by zeolite, some of which were subsequently released in the desorbing

Table 5
Comparison of the desorption efficiencies obtained for natural minerals in this work and in other studies.

Metal desorbed	Adsorbent	Desorbing solution	Desorption efficiency (1 cycle) (%)	Reference
Pb	Clinoptilolite	3 M KCl	>99.5	Present study
Zn	Clinoptilolite	1 M KCl	>98.5	Present study
Cd	Clinoptilolite	1 M NaCl	97	[10]
Pb	Clinoptilolite	0.5 NaCl	95	[11]
Zn	Clinoptilolite	0.34 M NaCl	24	[14]
Cu	Clinoptilolite	0.34 M NaCl	20	[14]
Zn	Clinoptilolite	5 g/l EDTA	29	[14]
Cu	Clinoptilolite	5 g/l EDTA	60	[14]
Zn	Bentonite	0.1 M HCl	98.5	[51]
Cu	Bentonite	0.1 M HCl	97.7	[51]
Co	Bentonite	0.1 M HCl	99.2	[51]
Cd	Goethite	0.01 M $Ca(NO_3)_2$	92	[52]
Ni	Clinoptilolite	0.1 M HCl	93	[53]
Cd	Clinoptilolite	0.1 M $KClO_3$	90	[54]
Cd	Clinoptilolite	1 M KNO_3	92	[54]

solution, thus limiting the actual desorption of lead from the solid phase into the solution. This was confirmed by occasional measurements of NH_4^+ and Na^+ in the desorbing solution. The above behaviour is explained by the cation selectivity sequence of the Na-form clinoptilolite where it is seen that NH_4^+, Na^+ and Pb^{2+} exhibited similar affinity to be adsorbed onto zeolite [47]. The lower desorption obtained when NaCl and NH_4Cl were used for the desorption of lead from zeolite eluted from MBR permeate compared to zeolite eluted from aqueous solutions was mainly attributed to the presence of sodium ions. Desorption efficiency was similar for zeolite eluted from all three liquid media when KCl was used since clinoptilolite exhibited high selectivity for potassium ions that were held by the mineral with strong bonds. This was confirmed by the cation selectivity order reported in the literature for natural clinoptilolite: $K^+ > NH_4^+ > Na^+ > Ca^{2+} > Mg^{2+}$ [48]. The most effective desorbing agent was 3 M KCl resulting in very high (>99.5%) desorption of Pb(II) in all three liquid media where the adsorption had taken place. However, significant concentrations are required to achieve effective lead desorption.

In Fig. 6 the percentage desorption efficiency of zinc achieved by employing the solutions of HNO_3, KCl, NaCl and NH_4Cl is given. 1 M KCl was very effective (>98.5%) for zinc desorption from zeolite eluted from all three liquid media. NH_4Cl (0.1–3 M) performed well (>80%) for all the examined cases. The use of 1 M and 3 M NaCl was effective (>80%) for zinc desorption from zeolite eluted from all three liquid media. The liquid medium where the adsorption process had taken place was not that critical for zinc desorption, as was the case for lead. It seems that the ammonium and sodium ions contained in wastewater and permeate were retained onto the mineral surface and interior by stronger bonds compared to zinc and could not be easily desorbed.

As seen in Figs. 5 and 6 the increase of the desorbing solution concentration enhanced the desorption process for both lead and zinc. The increase in ionic strength resulted in a subsequent increase of the desorption efficiency. This effect could be ascribed to the competition among the cations in the solution for the available adsorption sites, thus increasing the potential removal of lead and zinc ions from the solid to the liquid phase [49]. In particular, the

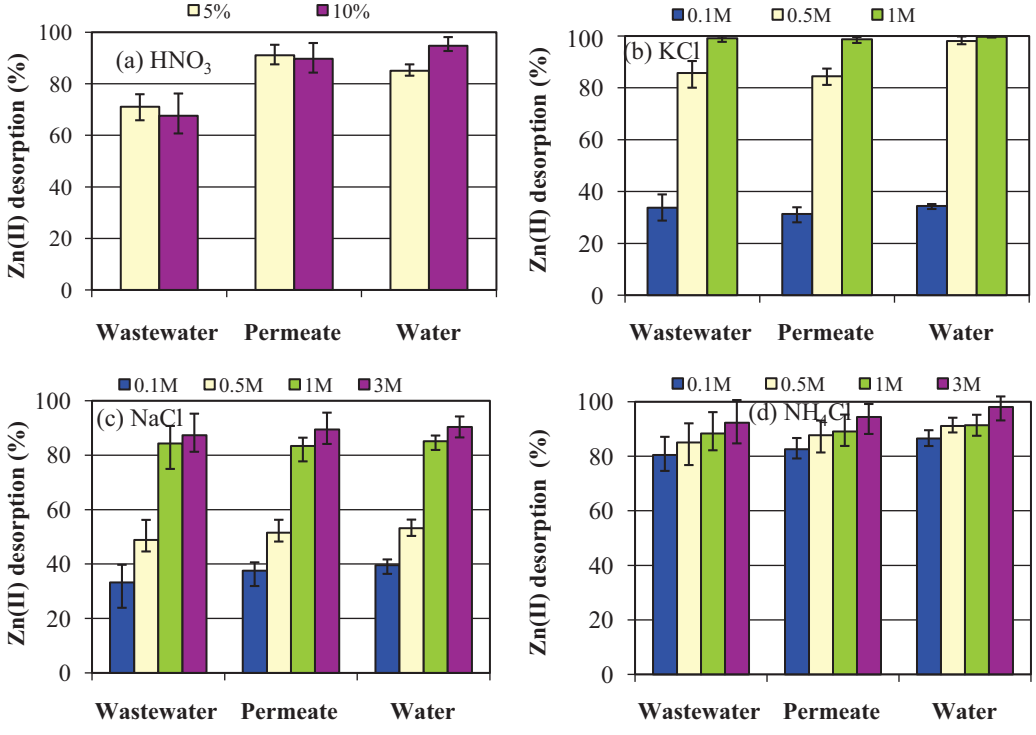

Fig. 6. Percentage desorption efficiency of Zn(II) achieved by (a) HNO_3, (b) KCl, (c) NaCl and (d) NH_4Cl.

Table 6
Kinetic parameters for the desorption of Pb(II) and Zn(II) into solution 3 M KCl and 1 M KCl respectively from zeolite eluted from aqueous solutions, permeate and wastewater.

Elution liquid medium	Pseudo-first-order			Pseudo-second-order			Elovich			Experimental
	k_{1d} (min^{-1})	q_d ($mg\,g^{-1}$)	Δq (%)	k_{2d} ($g\,mg^{-1}\,min^{-1}$)	q_d ($mg\,g^{-1}$)	Δq (%)	α ($mg\,g^{-1}\,min^{-1}$)	β ($g\,mg^{-1}$)	Δq (%)	q_{ed} ($mg\,g^{-1}$)
Pb(II)										
Water	0.00415	0.01	24.35	20.45×10^{-4}	0.00	65.98	0.167	0.144	11.76	0.29
Permeate	0.00425	0.03	26.09	22.27×10^{-4}	0.00	66.16	0.306	0.219	20.65	0.23
Wastewater	0.00405	0.03	24.69	20.19×10^{-4}	0.00	64.46	0.101	0.136	11.12	0.24
Zn(II)										
Water	0.00507	0.31	16.56	18.25×10^{-4}	0.00	40.62	0.231	0.350	12.29	0.40
Permeate	0.00585	0.27	19.91	24.79×10^{-4}	0.00	42.60	0.162	0.345	11.57	0.32
Wastewater	0.00483	0.38	19.41	16.77×10^{-4}	0.00	36.24	0.075	0.357	12.91	0.48

Elution liquid medium	Pb(II) parabolic Diffusion				Zn(II) parabolic Diffusion			
	k_{id1} ($mg\,g^{-1}\,min^{-1/2}$)	k_{id2} ($mg\,g^{-1}\,min^{-1/2}$)	$R_1{}^2$	$R_2{}^2$	k_{id1} ($mg\,g^{-1}\,min^{-1/2}$)	k_{id2} ($mg\,g^{-1}\,min^{-1/2}$)	$R_1{}^2$	$R_2{}^2$
Water	0.8897	0.1120	0.9973	0.6911	0.5059	0.0313	0.9950	0.8286
Permeate	0.8001	0.0684	0.9961	0.8984	0.4909	0.0118	0.9955	0.9956
Wastewater	0.7858	0.0993	0.9971	0.9000	0.3945	0.0168	0.9942	0.8319

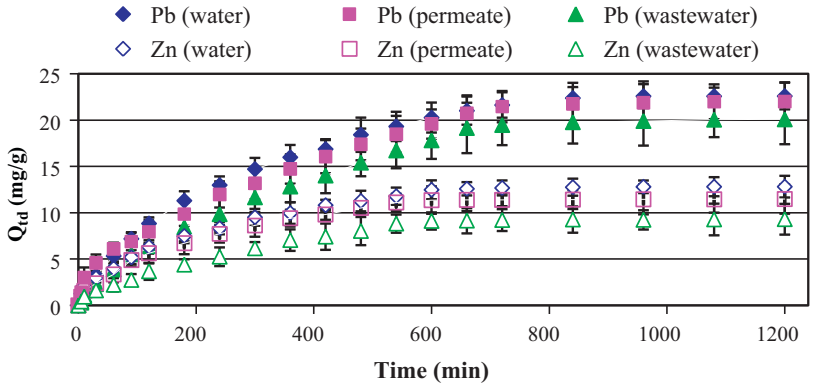

Fig. 7. Amount (mg/g) of lead and zinc desorbed from zeolite versus time using 3 M and 1 M KCl desorbing solutions, respectively.

increase in ionic strength means that more cations (Na^+, K^+, NH_4^+, H^+) were available in the desorbing solution and competed for the adsorption sites. Furthermore, high ionic strength favoured the formation of complexes among the desorbed metals and the chlorides present in the desorbing solution. The presence of salts could compress the electric double layer which surrounded the negatively charged surfaces, thus facilitating the desorption of lead and zinc [49,50]. In the case of NH_4Cl the increase of solution concentration also resulted in a reduction of the pH, thus further enhancing the desorption process.

An exception to the above behaviour was observed when the concentration of NaCl and NH_4Cl increased from 3 M to 5 M. The desorption efficiency reached a certain peak with increasing solution concentration and then reduced. At very high concentrations (5 M) it seems that despite the high amount of cations present in the solution, these are not effectively exchanged with the heavy metals adsorbed on the mineral. This could be attributed to the precipitation of lead chloride in the form of inner sphere complexes inside the cavities and channels of the mineral which were not easily removed, thus reducing the efficiency of the desorption process.

Comparing the desorption efficiency between zinc and lead for the same desorbing solution, it is deduced that lower concentrations of desorbing solution were required for the effective removal of Zn(II). Mineral performance was lower for zinc, but its release from the solid to the liquid phase was easier, showing the preference of zinc for the solution phase. Potassium chloride was found to be the best desorbent, indicating that zeolite is very selective for K^+ [48].

According to the obtained results, desorption depended on the type and concentration of the desorbing solution, the type of metal as well as the liquid medium where the adsorption process had taken place. In most cases, the desorbing solutions desorbed zinc more effectively than lead, although the adsorption of Pb(II) on of zeolite was higher. The most effective solution for zinc desorption was 1 M KCl and for lead it was 3 M KCl. Table 5 summarizes the desorption efficiencies reported in the literature for various minerals, metals and desorbing solutions [10,11,14,51–54]. It is evident that the desorption efficiencies obtained in this study for lead and zinc were very high (>98.5%).

Fig. 7 shows the amount of Pb(II) and Zn(II) desorbed with time from zeolite eluted from aqueous solutions, MBR permeate and wastewater. The desorbing solution employed was 3 M KCl for lead and 1 M KCl for zinc. It is clearly seen that desorption was much slower than adsorption since it required approximately 600 min to reach a state of equilibrium for zinc and 840 min for lead. Longer time was required for lead compared to zinc to reach equilibrium (which previously exhibited the highest adsorption onto zeolite), despite the fact that lead desorption rate was higher. Kinetic models were compared to the experimental data of desorption and the calculated constants are given in Table 6. The pseudo-second-order model could not adequately predict q_d, as it resulted in negative values. Since this has no physical meaning, the equation was solved for $q_d \geq 0$, thus predicting $q_d = 0$ in all cases. However, the associated error $\Delta q(\%)$ was large. The Elovich model provided the best fit to the experimental data. The plot of Q_{td} versus $t^{1/2}$ was employed to determine the rate limiting step of the process. A two-stage diffusion process was identified as opposed to the three-stage process of adsorption (Fig. 8). Metal desorption was gradual indicating desorption from the zeolite mesopores and micropores, while the second plot was associated with equilibrium. This is also confirmed by the fact that the rate constants of the second portion of the adsorption plot were comparable to those of the first plot of the desorption process. The main conclusion is that the desorption process was much slower than the adsorption process. Furthermore, it was more difficult for the ions that had been easily adsorbed on the mineral to be desorbed. The rate of metal desorption from zeolite eluted from aqueous solution was higher compared to that obtained for zeolite eluted from MBR permeate and wastewater.

4.4. Regeneration cycles

Several adsorption/desorption cycles (exceeding ten) were conducted for lead and zinc to determine the adsorption/desorption potential of the mineral, once it had been regenerated several times. The desorbent employed was 1 M KCl for zinc and 3 M KCl for lead, since these solutions exhibited the highest desorption performance. In Fig. 9a and b lead adsorption and desorption are given respectively for twelve regeneration cycles, while the respective amounts of zinc adsorbed/desorbed are given in Fig. 10a and b. These values were always obtained at equilibrium conditions. During the first three adsorption/desorption cycles the amount of metal adsorbed on the mineral was enhanced since the use of KCl enhanced the metal adsorption on zeolite. This finding agrees with previous research work [14]. Several reasons can account for this behaviour. Firstly, the removal of impurities (such as carbonates and sulphates) from the channels of the zeolite might allow more metals to reach the ion exchange sites. Furthermore, the KCl solution could modify the mineral structure by replacing ions originally present in the mineral (Ca^{2+}, Na^+, Mg^{2+}) with potassium ions present in the desorbing solution. The replacement of the above cations by potassium ions could enhance the mineral performance with respect to metal removal during the initial regeneration cycles. Furthermore, the increase of metal uptake could be attributed to the formation of complexes among chlorides and metals. In particular, during the desorption process chloride ions could be entrapped in the channels or cavities of clinoptilolite and

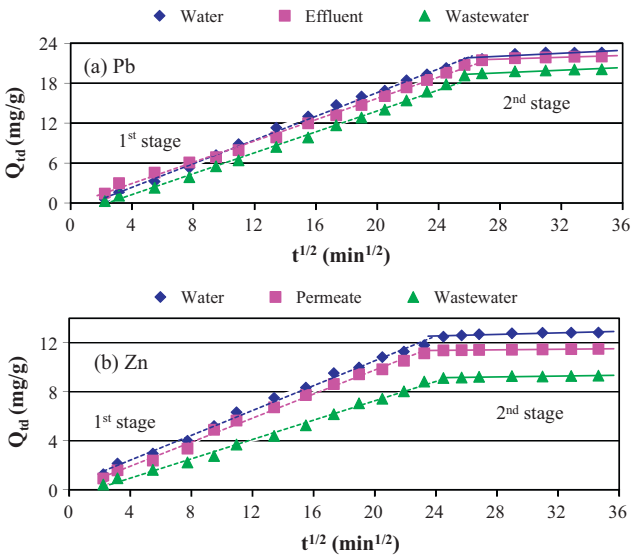

Fig. 8. Amount of (a) lead and (b) zinc desorbed from zeolite versus the square root of time using 3 M and 1 M KCl desorbing solutions, respectively.

remain there even after mineral washing. These ions could form inner sphere complexes with lead and zinc ions during the adsorption process and thus increase the overall removal of these metals [10,55]. The regeneration efficiency reduced with increasing number of regeneration cycles. This behaviour was observed for both zinc and lead. Inner sphere complexation was irreversible due to the formation of covalent bonds. As a result the desorption efficiency decreased with ascending adsorption/desorption cycles. The reduction in desorption efficiency during each cycle means that some heavy metals actually remained on the mineral and therefore decreased the amount of metal adsorbed during the subsequent adsorption cycles.

In the case of zinc the decrease in adsorption/desorption capacity with increasing cycles was more abrupt compared to that of lead. Regeneration efficiency for lead reduced within the first 3 cycles to approximately 80–85% and to less than 50% after 9 regeneration cycles. In the case of zinc the abrupt reduction of regeneration efficiency resulted in recovery rates lower than 50% in 4 adsorp-

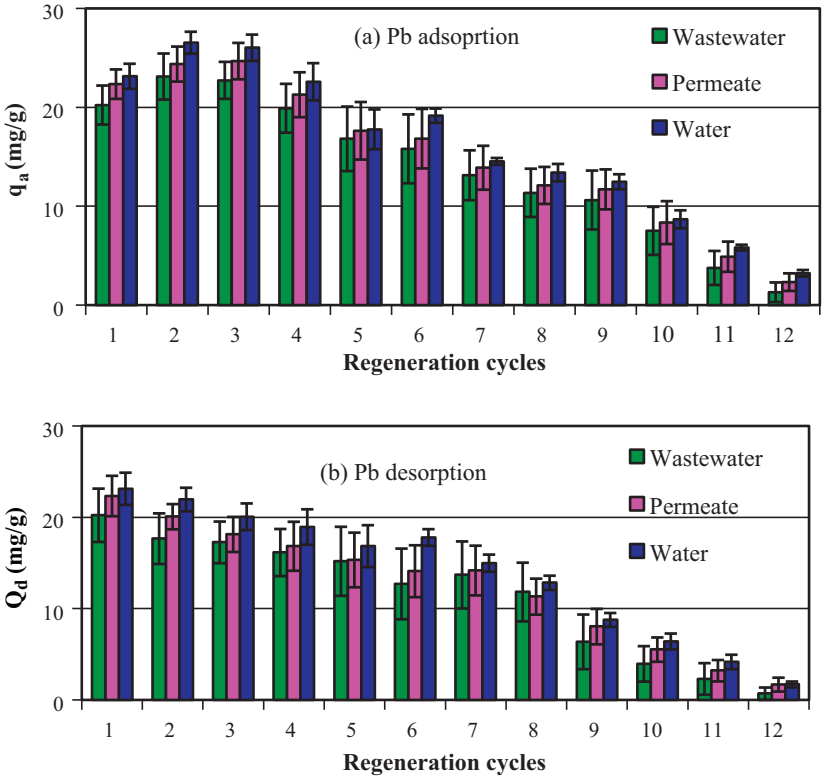

Fig. 9. Amount (mg/g) of Pb(II) (a) adsorbed and (b) desorbed during successive regeneration cycles.

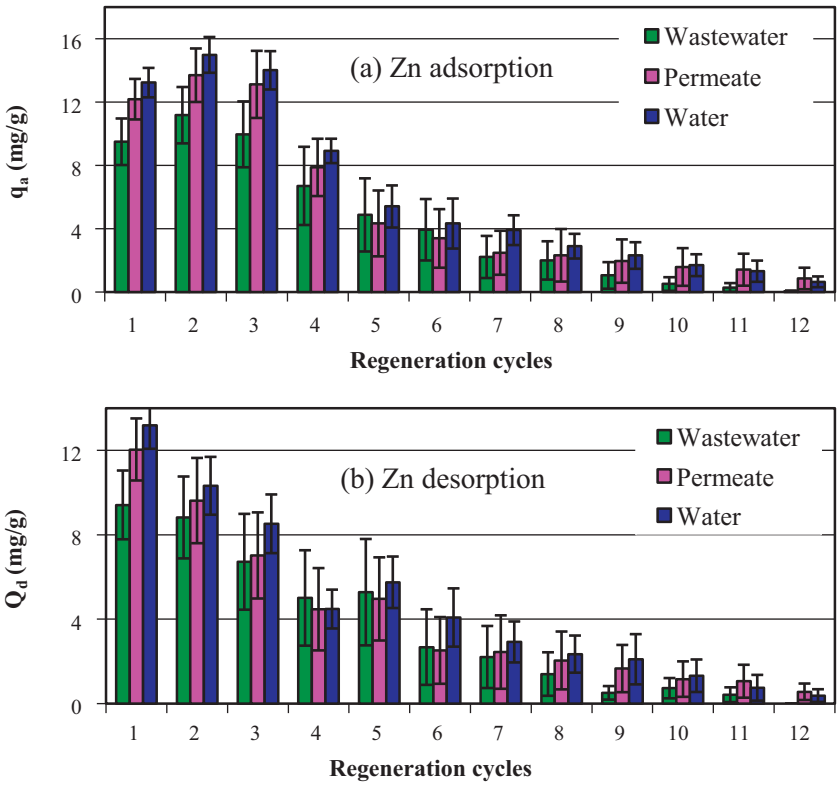

Fig. 10. Amount (mg/g) of Zn(II) (a) adsorbed and (b) desorbed during successive regeneration cycles.

tion/desorption cycles. The worse performance of zinc compared to lead can be attributed to the lower amount of zinc that had been adsorbed by zeolite and was thus available for the desorption process (Fig. 2). It seems that it was more difficult to achieve higher regeneration efficiencies for lower metal concentrations. Zeolite eluted from aqueous solution performed better compared to zeolite eluted from wastewater and MBR effluent, indicating that the liquid media in which adsorption had taken place influenced the subsequent regeneration. Although regeneration efficiency decreased significantly with ascending cycles, zeolite maintained part of its adsorption potential, particularly in the case of lead. The amount of lead adsorbed on zeolite at the 9th cycle was greater than 10 mg/g for all three liquid media, since more than 100 mg/l of lead ions could be removed from the solution. In some cases (e.g. 6th cycle for lead, 5th cycle for zinc) the desorption of Pb(II) and Zn(II) exceeded the adsorption for a given cycle. This was probably attributed to changes in mineral surface or mineral structure by the potassium captured during the successive adsorption/desorption cycles.

5. Conclusions

Adsorption was influenced by the type of sorbate and the nature of the solution, following the order aqueous solution > MBR permeate > wastewater. The desorption process depended on the type and concentration of the desorbing solution, the metal being desorbed and the liquid medium where the adsorption process had taken place. The results showed that for most desorbing solutions zinc was more effectively desorbed than lead. KCl was the most effective solution for the desorption process exhibiting very high desorption efficiencies (>98.5%) for both metals. In some cases the liquid media where the adsorption process had been conducted critically affected the desorption process, since lower performance was obtained for zeolite eluted from wastewater. Successive regeneration cycles resulted in significant reduction (>50%) of desorption efficiency after 9 and 4 cycles for lead and zinc, respectively. The desorption process was much slower than adsorption, while it was more difficult for the ions that were easily adsorbed to be desorbed. Adsorption was characterized by a three-stage diffusion process while desorption exhibited a two-stage diffusion process.

Acknowledgments

The authors would like to express their appreciation to the European Social Fund of the European Union and to the Ministry of Education, Lifelong Learning and Religious Affairs of Greece for financing this research in the framework of HERACLITUS II.

European Union
European Social Fund
OPERATIONAL PROGRAMME EDUCATION AND LIFELONG LEARNING
investing in knowledge society
MINISTRY OF EDUCATION, LIFELONG LEARNING AND RELIGIOUS AFFAIRS
MANAGING AUTHORITY
NSRF 2007-2013
EUROPEAN SOCIAL FUND
Co- financed by Greece and the European Union

References

[1] J. Rubio, M.L. Souza, R.W. Smith, Overview of flotation as a wastewater treatment technique, Miner. Eng. 15 (2002) 139–155.
[2] T.A. Kurniawan, G.Y.S. Chan, W.-H. Lo, S. Babel, Comparisons of low-cost adsorbents for treating wastewaters laden with heavy metals, Sci. Total Environ. 366 (2006) 409–426.
[3] S.O. Lesmana, N. Febriana, F.E. Soetaredjo, J. Sunarso, S. Ismadji, Studies on potential applications of biomass for the separation of heavy metals from water and wastewater, Biochem. Eng. J. 44 (2009) 19–41.
[4] A. Dimirkou, M.K. Doula, Use of clinoptilolite and an Fe-overexchanged clinoptilolite in Zn^{2+} and Mn^{2+} removal from drinking water, Desalination 224 (2008) 280–292.
[5] P. Castaldi, L. Santona, S. Enzo, P. Melis, Sorption processes and XRD analysis of a natural zeolite exchanged with Pb^{2+}, Cd^{2+} and Zn^{2+} cations, J. Hazard. Mater. 156 (2008) 428–434.
[6] A. Günay, E. Arslankaya, I. Tosun, Lead removal from aqueous solution by natural and pre-treated clinoptilolite: adsorption equilibrium and kinetics, J. Hazard. Mater. 146 (2007) 362–371.
[7] M. Sprynskyy, B. Buszewski, A.P. Terzyk, J. Namieśnik, Study of the selection mechanism of heavy metal (Pb^{2+}, Cu^{2+}, Ni^{2+} and Cd^{2+}) adsorption on clinoptilolite, J. Colloid Interface Sci. 304 (2006) 21–28.

[8] A. Cincotti, A. Mameli, A.M. Locci, R. Orru, G. Cao, Heavy metals uptake by Sardinian natural zeolites: experiment and modelling, Ind. Eng. Chem. Res. 45 (2006) 1074–1084.
[9] O. Oter, H. Akcay, Use of natural clinoptilolite to improve, water quality: sorption and selectivity studies of lead(II), copper(II), zinc(II), and nickel(II), Water Environ. Res. 79 (2007) 329–335.
[10] K. Gedik, I. Imamoglu, Removal of cadmium from aqueous solutions using clinoptilolite: influence of pretreatment and regeneration, J. Hazard. Mater. 155 (2008) 385–392.
[11] M. Turan, U. Mart, B. Yuksel, M.S. Celik, Lead removal in fixed-bed columns by zeolite and sepiolite, Chemosphere 60 (2005) 1487–1492.
[12] N.V. Medvidović, J. Peric, M. Trgo, Column performance in lead removal from aqueous solutions by fixed bed of natural zeolite-clinoptilolite, Sep. Purif. Technol. 49 (2006) 237–244.
[13] H. Cui, L.Y. Li, J.R. Grace, Exploration of remediation of acid rock drainage with clinoptilolite as sorbent in a slurry bubble column for both heavy metal capture and regeneration, Water Res. 40 (2006) 3359–3366.
[14] L.Y. Li, M. Chen, J.R. Grace, K. Tazaki, K. Shiraki, R. Asada, H. Watanabe, Remediation of acid rock drainage by regenerable natural clinoptilolite, Water Air Soil Pollut. 180 (2007) 11–27.
[15] APHA, Standard Methods for the Examination of Water and Wastewater, 20th ed., American Public Health Association, American Water Works Association, Water Environment Federation, Washington, DC, 1998.
[16] D.L. Sparks, Kinetics of Soil Chemical Processes, Academic Press, San Diego, CA, 1989.
[17] M.I. Zaman, S. Mustafa, S. Khan, B. Xing, Heavy metal desorption kinetic as affected by of anions complexation onto manganese dioxide surfaces, Chemosphere 77 (2009) 747–755.
[18] S. Lagergren, Zur theorie der sogenannten adsorption gelöster stoffe, Kungliga Svenska Vetenskapsakademiens, Handlingar 24 (1898) 1–39.
[19] J.-Y. Tseng, C.-Y. Chang, C.-F. Chang, Y.-H. Chen, C.-C. Chang, D.-R. Ji, C.-Y. Chiu, P.-C. Chiang, Kinetics and equilibrium of desorption removal of copper from magnetic polymer adsorbent, J. Hazard. Mater. 171 (2009) 370–377.
[20] Y.S. Ho, Adsorption of heavy metals from waste streams by peat, Ph.D. Dissertation, University of Birmingham, UK, 1995.
[21] R.L. Tseng, F.C. Wu, R.S. Juang, Liquid-phase adsorption of dyes and phenols using pinewood-based activated carbons, Carbon 41 (2003) 487–495.
[22] E. Guibal, C. Milot, J.M. Tobin, Metal-anion sorption by chitosan beads: equilibrium and kinetic studies, Ind. Eng. Chem. Res. 37 (1998) 1454–1463.
[23] D. Reichenberg, Properties of ion-exchange resin in relation to their structure III. Kinetics of exchange, J. Am. Chem. Soc. 75 (1953) 589–597.
[24] M. Trgo, J. Perić, N. Vukojević Medvidović, A comparative study of ion exchange kinetics in zinc/lead-modified zeolite-clinoptilolite systems, J. Hazard. Mater. B136 (2006) 938–945.
[25] J. Shen, Z. Duvnjak, Adsorption kinetics of cupric and cadmium ions on corncob particles, Process Biochem. 40 (2005) 3446–3454.
[26] Z. Cheng, X. Liu, M. Han, W. Ma, Adsorption kinetic character of copper ions onto a modified chitosan transparent thin membrane from aqueous solution, J. Hazard. Mater. 182 (2010) 408–415.
[27] G.M. Walker, L. Hansen, J.A. Hanna, S.J. Allen, Kinetics of a reactive dye adsorption onto dolomitic sorbents, Water Res. 37 (2003) 2081–2089.
[28] M.A. Stylianou, V.J. Inglezakis, K.G. Moustakas, S.P. Malamis, M.D. Loizidou, Removal of Cu(II) in fixed bed and batch reactors using natural zeolite and exfoliated vermiculite as adsorbents, Desalination 215 (2007) 133–142.
[29] S.T. Bosso, J. Enzweiler, Evaluation of heavy metal removal from aqueous solution onto scolecite, Water Res. 36 (2002) 4795–4800.
[30] A.E. Turkman, S. Aslan, I. Ege, Treatment of metal containing wastewaters by natural zeolites, Fresenius Environ. Bull. 13 (2004) 574–580.
[31] N. Bektas, S. Kara, Removal of lead from aqueous solutions by natural clinoptilolite: equilibrium and kinetic studies, Sep. Purif. Technol. 39 (2004) 189–200.
[32] A. Günay, E. Arslankaya, I. Tosun, Lead removal from aqueous solution by natural and pretreated clinoptilolite: adsorption equilibrium and kinetics, J. Hazard. Mater. 146 (2007) 362–371.
[33] S.S. Gupta, K.G. Bhattacharyya, Interaction of metal ions with clays: I. A case study with Pb(II), Appl. Clay Sci. 30 (2005) 199–208.
[34] Y. Liu, D. Xiao, H. Li, Kinetics and thermodynamics of lead(II) adsorption on vermiculite, Sep. Sci. Technol. 42 (2007) 185–202.
[35] E.F. Covelo, F.A. Vega, M.L. Andrade, Competitive sorption and desorption of heavy metals by individual soil components, J. Hazard. Mater. 140 (2007) 308–315.
[36] R. Naseem, S.S. Tahir, Removal of Pb(II) from aqueous/acidic solutions by using bentonite as an adsorbent, Water Res. 35 (2001) 3982–3986.
[37] A.R. Kul, H. Koyuncu, Adsorption of Pb(II) ions from aqueous solution by native and activated bentonite: kinetic, equilibrium and thermodynamic study, J. Hazard. Mater. 179 (2010) 332–339.
[38] E. Eren, B. Afsin, Y. Onal, Removal of lead ions by acid activated and manganese oxide-coated bentonite, J. Hazard. Mater. 161 (2009) 677–685.
[39] A. Kaya, A.H. Ören, Adsorption of zinc from aqueous solutions to bentonite, J. Hazard. Mater. 125 (2005) 183–189.
[40] S.H. Lin, R.S. Juang, Heavy metal removal from water by sorption using surfactant-modified montmorillonite, J. Hazard. Mater. 92 (2002) 315–326.
[41] S. Veli, B. Alyüz, Adsorption of copper and zinc from aqueous solutions by using natural clay, J. Hazard. Mater. 149 (2007) 226–233.
[42] P.C. Mishra, R.K. Patel, Removal of lead and zinc ions from water by low cost adsorbents, J. Hazard. Mater. 168 (2009) 319–325.
[43] A. Mockovčiaková, Z. Orolínová, J. Škvarla, Enhancement of the bentonite sorption properties, J. Hazard. Mater. 180 (2010) 274–281.
[44] E. Alvarez-Ayuso, A. Garcia-Sanchez, X. Querol, Purification of metal electroplating waste waters using zeolites, Water Res. 37 (2003) 4855–4862.
[45] E. Erdem, N. Karapinar, R. Donat, The removal of heavy metal cations by natural zeolites, J. Colloid Interface Sci. 280 (2004) 309–314.
[46] V. Chantawong, N.W. Harvey, V.N. Bashkin, Comparison of heavy metal adsorption by Thai kaolin and ballclay, Water Air Soil Pollut. 148 (2003) 111–125.
[47] A. Langella, M. Pansini, P. Cappelletti, B. de Gennaro, M. de' Gennaro, C. Colella, NH_4^+, Cu^{2+}, Zn^{2+}, Cd^{2+} and Pb^{2+} exchange for Na^+ in a sedimentary clinoptilolite, North Sardinia, Italy, Micropor. Mesopor. Mater. 37 (2000) 337–343.
[48] A. Farkaš, M. Rožić, Z. Barbarić-Mikočević, Ammonium exchange in leakage waters of waste dumps using natural zeolite from the Krapina region, Croatia, J. Hazard. Mater. 117 (2005) 25–33.
[49] S. Yuan, Z. Xi, Y. Jiang, J. Wan, C. Wu, Z. Zheng, X. Lu, Desorption of copper and cadmium from soils enhanced by organic acids, Chemosphere 68 (2007) 1289–1297.
[50] Y.H. Xu, D.Y. Zhao, Removal of copper from contaminated soil by use of poly(amidoamine) dendrimers, Environ. Sci. Technol. 39 (2005) 2369–2375.
[51] T.S. Anirudhan, P.S. Suchithra, Heavy metals uptake from aqueous solutions and industrial wastewaters by humic acid-immobilized polymer/bentonite composite: kinetics and equilibrium modelling, Chem. Eng. J. 156 (2010) 146–156.
[52] G. Mustafa, R.S. Kookana, B. Singh, Desorption of cadmium from goethite: effects of pH, temperature and aging, Chemosphere 64 (2006) 856–865.
[53] M.E Argun, Use of clinoptilolite for the removal of nickel ions from water: kinetics and thermodynamics, J. Hazard. Mater. 150 (2008) 587–595.
[54] V.O. Vasylechko, G.V. Gryshchouk, Yu.B. Kuz'ma, V.P. Zakordonskiy, L.O. Vasylechko, L.O. Lebedynets, M.B. Kalytovs'ka, Adsorption of cadmium on acid-modified Transcarpathian clinoptilolite, Micropor. Mesopor. Mater. 60 (2003) 183–196.
[55] M.K. Doula, A. Ioannou, The effect of electrolyte anion on Cu adsorption-desorption by clinoptilolite, Micropor. Mesopor. Mater. 58 (2003) 115–130.